Theory of rapid-oscillation phenomena in the low-dimensional conductors $(TMTSF)_2X$

1997 J. Phys.: Condens. Matter 9 2211

(http://iopscience.iop.org/0953-8984/9/10/010)

J. Phys.: Condens. Matter **9** (1997) 2211–2224. Printed in the UK PII: S0953-8984(97)74062-1

Theory of rapid-oscillation phenomena in the low-dimensional conductors $(TMTSF)_2X$

Keita Kishigi† and Kazushige Machida‡

Department of Physics, Okayama University, Okayama 700, Japan

Received 29 April 1996, in final form 3 December 1996

Abstract. We analyse theoretically the so-called rapid-oscillation phenomena whose characteristics are quite different from those of the ordinary de Haas–van Alphen effect in the magnetization oscillation or the Shubnikov–de Haas effect in the magnetoresistance oscillation, observed in the low-dimensional conductors $(TMTSF)_2X$ ($X = PF_6, ClO_4, NO_3, ReO_4$ and AsF_6). By comparatively studying two systems that are very similar (those with $X = ClO_4$ and NO_3), yet with quite different rapid-oscillation features, we have identified the origin of the mysterious field and temperature dependence of the rapid oscillation. Direct diagonalization of the Hamiltonian matrices of the standard model under a field yields the magnetization. The subtle interplay between the anion ordering and spin-density-wave (SDW) ordering is found to be an important factor in the understanding of the quantum magnetic oscillations. We find a non-monotonic temperature dependence of the rapid-oscillation amplitude, which qualitatively agrees with the existing experiments. It is governed by two competing factors: the SDW-gap-closing effect in addition to the usual thermal broadening one. The former (latter) increases (diminishes) the rapid-oscillation amplitude with increasing temperature.

1. Introduction

Certain low-dimensional conductors, the Bechgaard salts $(TMTSF)_2X$ (tetramethyltetraselenafulvalene with $X = PF_6$, ClO_4, NO_3, ReO_4 and AsF_6) [1], are known to exhibit a variety of phase transitions due to the low dimensionality of their electronic structure. For $X = ClO_4$ and pressurized PF_6, the so-called field-induced spin-density wave (FISDW) occurs at low temperatures ($T \sim$ a few K) and above the threshold field ($H \sim$ a few T). As a function of the external field, the SDW wave number $Q_x = 2k_F + N\delta$ (k_F is the Fermi wave number and N is an integer) along the most highly conducting direction (the k_x-axis) of the SDW order parameter changes, and the corresponding subphases characterized by different N-values vary successively via first-order transitions.

This behaviour has been successfully explained by several authors [2] on the basis of the so-called standard model. The magnetic field tends to improve the incomplete-nesting situation of the original model band, which consists of a pair of parallel open surfaces as shown in figure 1(a), and drives the normal metallic state into a SDW state. The electron and hole pockets remaining after the SDW formation has occurred are quantized, and play an important role in stabilizing a particular subphase over a particular field and temperature domain. These electron and hole closed orbits are obtained from the imperfect nesting. Depending on the details of the subtle differences in the Fermi surfaces, the SDW can be

† kishigi@mp.okayama-u.ac.jp
‡ machida@mp.okayama-u.ac.jp

0953-8984/97/102211+14$19.50

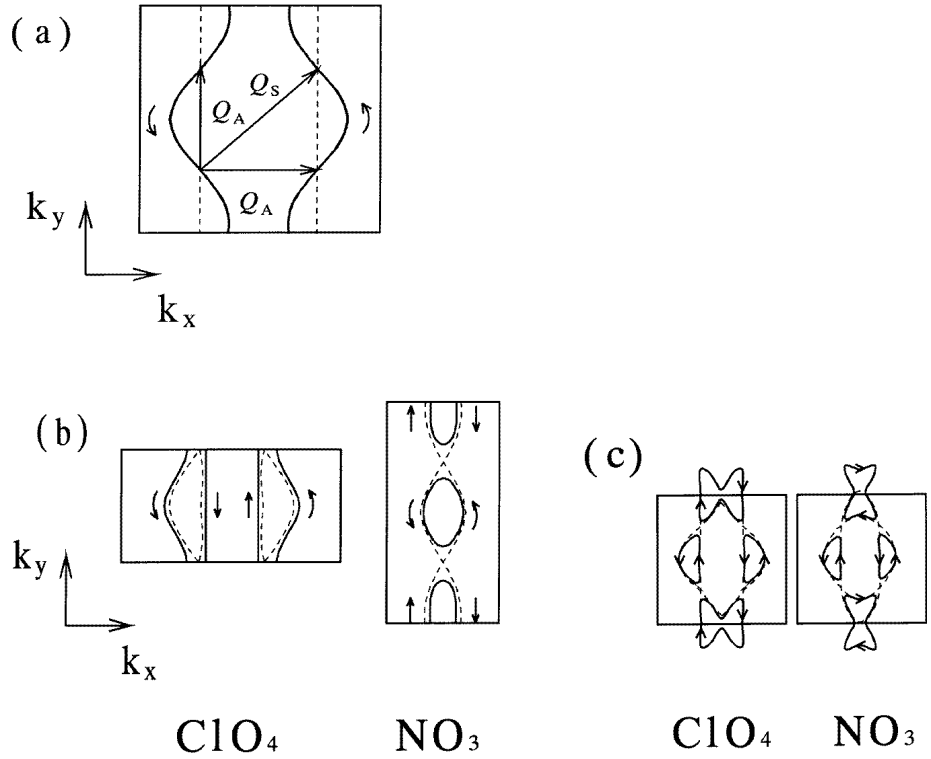

Figure 1. (a) A pair of open Fermi surfaces ($t_b/t_a = 0.6$ and $t'_b/t_a = 0.2$). The two $\boldsymbol{Q}_a$s for anion ordering correspond to $(0, \pi/b)$ for X = ClO_4 and $(\pi/a, 0)$ for X = NO_3. The SDW vector is $\boldsymbol{Q}_s = (\pi/a, \pi/b)$. (b) Fermi surfaces folded by the anion ordering (broken lines) and the resulting ones (bold lines) obtained when taking the anion-ordering potential into consideration ($t_b/t_a = 0.6$, $t'_b/t_a = 0.2$, and $v = 0.2$). The arrows indicate the sense of the orbital motion under a perpendicular field. (c) Fermi surfaces (bold lines) obtained when the anion ordering and SDW ordering exist simultaneously ($t_b/t_a = 0.6$, $t'_b/t_a = 0.2$, $v = 0.2$, and $\Delta = 0.03$) in the reduced zone scheme. Broken lines indicate closed orbits that are possible due to the magnetic breakdown, giving rise to the rapid oscillation. The closed orbits denoted by bold lines yield the slow oscillations for X = NO_3.

stabilized without any field H—such as for X = NO_3 where $T_{SDW} \sim 12$ K. Nevertheless, the SDW nesting for X = NO_3 does not become perfect, because of it having the band parameter common for all $(TMTSF)_2X$ compounds.

Over a wide region of T and H, the quantum magnetic oscillations called rapid oscillations are observed in some of these systems (those with X = PF_6 [3], ClO_4 [4–10], NO_3 [11, 12], ReO_4 [13], and AsF_6 [14]); the rapid-oscillation frequencies in these systems are similar (∼260 T). The rapid-oscillation phenomena are quite distinct from the ordinary Shubnikov–de Haas (SdH) phenomena in transport properties such as the magnetoresistance $\rho(H)$, and the de Haas–van Alphen (dHvA) oscillation in thermodynamic quantities, in important and fundamental ways. Recently, remarkable experiments have been done for X = NO_3 [12] and X = ClO_4 [10], which might enable us to explain the rapid-oscillation phenomena in a coherent manner. The puzzles associated with the rapid oscillation are summarized as follows [15].

(1) A rapid oscillation for X = NO_3 is observed in $\rho(H)$ at low T below the anion-ordering temperature $T_{AO} = 45$ K whose characteristic ordering vector $\boldsymbol{Q}_a = (\pi/a, 0)$ (a and b are the lattice constants of the two-dimensional (x, y) conducting plane). The T-dependence of the Fourier-transformed amplitude, $A_{RO}(T)$, of the rapid oscillation whose frequency $F_{RO} = 249$ T has a maximum at $T \sim 4$ K, and the oscillation ceases to be observed at lower T, which is not expected for the ordinary SdH effect.

(2) For X = ClO_4 the rapid oscillation of thermodynamic quantities such as the magnetization M [6] and the specific heat is observed [9] only in the SDW phase, while the transport quantities [5, 10], e.g. $\rho(H)$, exhibit the rapid oscillation throughout the low-T and high-H region below $T_{AO} = 24$ K whose characteristic ordering vector $\boldsymbol{Q}_a = (0, \pi/b)$. Yet the observed rapid-oscillation frequencies ($F_{RO} = 260$ T) in both measurements are identical even when the SDW boundary is crossed. The oscillation wave forms in $\rho(H)$ above and below $T = T_{SDW}$ change dramatically from a simple sinusoidal form to a non-sinusoidal one with several higher harmonics [10]. Again the rapid oscillation mysteriously disappears upon further lowering T: the intensity has a peak structure as a function of T, giving rise to a maximum just below T_{SDW} [10].

(3) For X = NO_3, in addition to the rapid oscillation with $F_{RO} = 249$ T, another oscillation with lower frequency, $F_{LO} = 67$ T, is also observed [12] in $\rho(H)$. The intensity of this oscillation is a decreasing function of H. This contrasts with the above $A_{RO}(H)$, which increases as H increases.

(4) The rapid oscillation for X = ClO_4 disappears when the anion ordering is removed by applying a moderate pressure [16]. Therefore the anion ordering is indispensable for the rapid-oscillation phenomena to occur. The rapid oscillations, however, are also found for compounds with X = PF_6 and X = AsF_6; in such compounds the anion ordering is absent. In our theory based on the anion ordering, we cannot explain the rapid oscillations in these systems. (See the note added in proof.)

Although some of these phenomena, collectively called rapid-oscillation phenomena, have been considered theoretically [17], none of the studies have succeeded in giving a coherent picture explaining these remarkable facts. These facts are related to the fundamental problems of the quantum magnetic oscillations in general under extreme conditions of high H and low T. These have not been fully explained from first principles.

The purpose of this paper is to give the essence of the physics involved, to enable us to explain these phenomena coherently. Specifically, we will try to explain the two main mysteries as regards the rapid oscillation.

(i) Why is the thermodynamic oscillation confined to the SDW region for X = ClO_4?

(ii) Why does the intensity of the rapid oscillation exhibit anomalous H- and T-dependences both for X = ClO_4 and for X = NO_3?

Our strategy is just to evaluate fully quantum mechanically the energy of the system as a function of H and to calculate, for example, the magnetization for the established band model, or the so-called 'standard model Hamiltonian', which is known to be successful in explaining various properties of the Bechgaard salts—in particular, the field-induced SDW transition [1, 2]. This paper is one of a series of papers [18, 19] in which we have been investigating the magnetic quantum oscillations associated with the magnetic breakdown effect from first principles, and trying to establish a general framework for the quantum oscillations. So far our strategy has been quite successful, and has recovered the semi-classical picture embodied by the Lifshitz and Kosevich (LK) formula [20, 21] for describing the dHvA effect where it is applicable.

In the next section we explain the Fermi surfaces for both X = ClO_4 and X = NO_3

in order to facilitate the understanding of the possible magnetic oscillations. After giving a formulation in section 3, we calculate the magnetization $M(H)$ at $T = 0$ in section 4. The temperature dependence of the rapid-oscillation amplitude is investigated in section 5. The final section is devoted to discussions and a summary [22].

2. Fermi surface situations for X = ClO_4 and X = NO_3

Before going into the detailed formulation of our problem, we look into the actual Fermi surface situations for X = ClO_4 and X = NO_3 in order to achieve an understanding of how these two systems are similar and different. The standard model is an anisotropic Hubbard Hamiltonian consisting of

$$\mathcal{H}_0 = -\frac{1}{2}\sum_{i,j,\sigma} t_{i,j} C^{\dagger}_{i\sigma} C_{j\sigma} \tag{1}$$

and

$$\mathcal{H}_{\rm int} = \frac{U}{2}\sum_{i,j,\sigma} n_{i\sigma} n_{j-\sigma} \tag{2}$$

where $C^{\dagger}_{i\sigma}$ is the creation operator of an electron at site i with the spin σ in two dimensions. The Fourier transform of the hopping integral $t_{i,j}$ yields the standard model band:

$$\epsilon(k_x, k_y) = -t_a \cos k_x a - t_b \cos k_y b - t'_b \cos 2k_y b \tag{3}$$

where $t_a > t_b > t'_b$; thus the k_x-direction is the most highly conducting one. In what follows the energy is measured in units of t_a.

Let us look carefully into the nature of the anion ordering in two systems. The effect of anion ordering may be expressed as

$$\mathcal{H}_{\rm AO} = V\sum_{\boldsymbol{k},\sigma}(C^{\dagger}_{\boldsymbol{k}+\boldsymbol{Q}_a\sigma} C_{\boldsymbol{k}\sigma} + {\rm HC}) \tag{4}$$

where $\boldsymbol{Q}_a$ is the anion-ordering vector. The anion-ordering potential v is normalized as $v = V/t_a$. The Fermi surface consisting of two nearly parallel open sheets, as shown in figure 1, is folded back by the respective ordering vectors: $(0, \pi/b)$ for X = ClO_4 and $(\pi/a, 0)$ for X = NO_3, giving rise to similar folded Fermi surfaces as shown using broken lines of figure 1(b). The sense of the orbital motion denoted by an arrow when $\boldsymbol{H}$ is applied perpendicular to the conduction plane is the same (opposite) for X = ClO_4 (X = NO_3). The resulting Fermi surfaces are depicted using bold lines in figure 1(b), which were calculated by diagonalizing a 2×2 Hamiltonian matrix for $\mathcal{H}_0 + \mathcal{H}_{\rm AO}$. The degenerate states corresponding to the intersection points of the broken lines repel each other so as to give two parallel Fermi surfaces for X = ClO_4 or mix together to give two closed Fermi surfaces for X = NO_3. The former is an ideal situation for the Stark quantum interference oscillation for the transport properties [21, 23]; that is, the electron wave is split at a junction and then interferes at the next junction when the current flows along the y-axis. The oscillation is periodic against $1/H$ and proportional to the enclosed area, and the wave form is sinusoidal without any higher harmonics [23]. Yet these parallel orbits *never* give rise to the thermodynamic oscillation [24], because this would not obey the Onsager orbital quantization rule. As in the case for X = NO_3 shown in figure 1(b), since there exist two closed orbits with opposite senses—the electron and hole surfaces—both the thermodynamic and the transport quantities should show magnetic oscillation (dHvA or

SdH oscillation). This semi-metallic Fermi surface situation for X = NO_3 is indeed seen experimentally [25, 26].

Let us now consider the effect of the SDW formation on the reorganization of the Fermi surface whose nesting vector is approximated by $\boldsymbol{Q}_s = (2k_F, \pi/b)$. [27] Since the band filling is half-filling in this problem, $2k_F = \pi/a$. We discuss the filling shortly. In a mean-field approximation the interaction Hamiltonian $\mathcal{H}_{\rm int}$ in (2) is rewritten as

$$\mathcal{H}_{\rm SDW} = 2\tilde{\Delta} \sum_{\boldsymbol{k}} (C^{\dagger}_{\boldsymbol{k}+\boldsymbol{Q}_s\uparrow} C_{\boldsymbol{k}\downarrow} + {\rm HC}). \tag{5}$$

The SDW order parameter $\tilde{\Delta}$ is defined by a self-consistent equation:

$$\tilde{\Delta} = -U \sum_{\boldsymbol{k}} \langle C^{\dagger}_{\boldsymbol{k}\downarrow} C_{\boldsymbol{k}+\boldsymbol{Q}_s\uparrow} \rangle. \tag{6}$$

The order parameter Δ normalized by t_a ($\Delta = \tilde{\Delta}/t_a$) exerts a periodic potential that further reorganizes the electron band. The resulting Fermi surfaces are depicted in figure 1(c) for both X = ClO_4 and X = NO_3; they were calculated by diagonalizing a 4×4 Hamiltonian matrix for $\mathcal{H} = \mathcal{H}_0 + \mathcal{H}_{\rm AO} + \mathcal{H}_{\rm SDW}$. They are very similar. It is now evident that in the Fermi surface for X = ClO_4 there appear possible *closed orbits*—electron and hole pockets—depicted using broken lines in figure 1(c), whose areas are nearly equal to those for X = NO_3 when the external field is applied perpendicular to the plane. For X = NO_3 the closed orbits with the same sizes still persist even after the SDW is formed—this is shown in figure 1(c)—although the closed orbits are blocked by the SDW gaps formed at the crossing points of the broken lines in figure 1(c). In both Fermi surfaces there appear small additional electron and hole pockets, because the SDW nesting by $\boldsymbol{Q}_s$ is incomplete. These may give the additional oscillations, which will indeed be manifested in $M(H)$ as a slow oscillation.

We adopt the following principle when choosing the parameters: in the vicinity of the Fermi surface, the present systems are well described by the one-band model of (3) with $\frac{3}{4}$-filling [1]. In the real systems, however, the total band consists of a filled lower band and a half-filled upper band, because of the special arrangement of two TMTSF molecules in a unit cell. The relevant band is the upper one with half-filling, which is modified by the anion-ordering vectors $\boldsymbol{Q}_a = (\pi/a, 0)$ and $(0, \pi/b)$. Therefore, we focus entirely on this upper band described by (3). We choose the parameters t_a, t_b, and t_b' so that the topology of the Fermi surface—that is, a pair of parallel open sheets in figure 1(a)—is unchanged. Furthermore, although it is known that for the present systems t_a:t_b:t_b' = 1:0.1:0.01 when using the one-band model of (3) with $\frac{3}{4}$-filling, we use slightly different ratios for computational convenience (which tend to exaggerate the imperfect-nesting situation), but keep the topology of the Fermi surface unchanged; that is, the small closed orbits shown by the bold lines in figure 1(c) necessarily remain after the SDW ordering. These pockets are fully responsible for the dHvA oscillations via the magnetic breakdown orbits denoted using broken lines there, even if their areas are very small for real parameter values. The anion-ordering potential V and the SDW gap Δ are not known from experiment. In view of their respective transition temperatures, it is expected that $v > \Delta$ and also $t_b' \sim V$.

3. Formulation of the problem

In order to obtain the possible magnetic oscillations in characteristic T- and H-domains—namely, the normal metallic state with the anion ordering and the SDW state where the

anion and SDW ordering exist simultaneously—we diagonalize the following mean-field Hamiltonian to evaluate the free energy:

$$\mathcal{H} = \mathcal{H}_0 + \mathcal{H}_{\mathrm{AO}} + \mathcal{H}_{\mathrm{SDW}} \tag{7}$$

under an applied field; each of the components has been defined above.

The magnetic field applied perpendicular to the plane is introduced in a standard manner known as the Peierls substitution:

$$\boldsymbol{k} \to \boldsymbol{k} + \frac{e}{\hbar c}\boldsymbol{A} \tag{8}$$

using the Landau gauge $\boldsymbol{A} = (Hy, 0)$. The resulting kinetic Hamiltonian $\mathcal{H}_0$ is

$$-\frac{t_a}{2}\sum_{\boldsymbol{k},\sigma}\left\{\exp(\mathrm{i}ak_x)C^{\dagger}_{k_x,k_y-\delta\sigma}C_{\boldsymbol{k}\sigma} + \mathrm{HC}\right\} + \sum_{\boldsymbol{k},\sigma}\left\{-t_b\cos(k_y b)C^{\dagger}_{\boldsymbol{k}\sigma}C_{\boldsymbol{k}\sigma} - t'_b\cos(2k_y b)C^{\dagger}_{\boldsymbol{k}\sigma}C_{\boldsymbol{k}\sigma}\right\}. \tag{9}$$

Here,

$$\delta = \frac{eaH}{\hbar c} = \frac{\phi}{\phi_0}\frac{2\pi}{b} = h\frac{2\pi}{b}. \tag{10}$$

$\phi = abH$ is the flux passing through a unit cell, $\phi_0 = 2\pi\hbar c/e$ is the unit flux quantum, and

$$h = \frac{\phi}{\phi_0} \tag{11}$$

is the number of flux quanta per unit cell. We represent the magnetic field by h, henceforth.

The number of flux quanta per unit cell, $h = \phi/\phi_0$, must be a rational number for periodic boundary conditions. That is, h is p/q, where p and q are mutually prime numbers. As a result, the Hamiltonian matrix size becomes $2p \times 2p$, where the factor 2 comes from the SDW ordering along the k_x-direction. We select many discrete hs where p and q are less than 500. When we assume $a \simeq 7.2$ Å and $b \simeq 7.7$ Å, $h \simeq 1/500$ corresponds nearly to 20 T, which becomes an almost realistic value. The number of lattice sites N_{sys} is determined by N^x_{sys} (N^y_{sys}) for the k_x-direction (k_y-direction). In our calculations, we have chosen $N^x_{\mathrm{sys}} \simeq 150$ and $N^y_{\mathrm{sys}} \simeq 1000$. By diagonalizing the Hamiltonian under the periodic boundary conditions, the energy eigenvalues ε^h_l obtained give the total ground-state energy per site $E(h)$ through

$$E(h) = \frac{1}{N_{\mathrm{sys}}}\sum_{l=1}^{nN_{\mathrm{sys}}}\varepsilon^h_l \tag{12}$$

where the index l is numbered from the lowest energy level. In the present systems, the number of electrons per site n is $\frac{1}{2}$. The magnetization is evaluated by numerically differentiating (12) with respect to h, where we have taken $\mu_B = 1$, i.e. $M(h) = -\partial E(h)/\partial h$.

For the Fourier transformation, we have used the following procedure: the Fourier-transformed amplitude $A_f \equiv |M(f)|^2$ for the frequency f is determined through

$$M(f) = \frac{1}{2L}\int_{h_c^{-1}-L}^{h_c^{-1}+L} M(h)\mathrm{e}^{\mathrm{i}\,2\pi Fh^{-1}}\,\mathrm{d}\left(\frac{1}{h}\right) \tag{13}$$

where $2L$ is the width of the Fourier window and h_c^{-1} is its centre. The field dependence of $A_f(h)$ arises through h_c^{-1}. The oscillation frequency f corresponds to S/S_{BZ}, where S is the area of the closed orbit and $S_{\mathrm{BZ}} = 4\pi^2/ab$ is the area of the first Brillouin zone [18].

The method of calculation for the magnetization at finite temperatures is the same as before [18]: for a given $\Delta(T)$ at a certain T we diagonalize $\mathcal{H} = \mathcal{H}_0 + \mathcal{H}_{\rm AO} + \mathcal{H}_{\rm SDW}$ to obtain the (one-body) energy eigenvalues ε_l^h. From the energy eigenvalues obtained, the magnetization is calculated for a given magnetic field h, temperature T, and number of electrons per site $n = \frac{1}{2}$, as follows. First, we derive the chemical potential $\mu(h, T)$ by inverting

$$n = \frac{1}{N_{\rm sys}} \sum_{l=1}^{N_{\rm sys}} \left[\exp\left(\frac{\varepsilon_l^h - \mu}{T} \right) + 1 \right]^{-1}. \tag{14}$$

Second, we calculate the free energy per site $F(h, T)$ from

$$F = \mu n - \frac{T}{N_{\rm sys}} \sum_{l=1}^{N_{\rm sys}} \log \left\{ \exp\left(\frac{\mu - \varepsilon_l^h}{T} \right) + 1 \right\} \tag{15}$$

which reduces to equation (12) when $T = 0$. We obtain the magnetization $M(h, T)$ by numerically differentiating: $M(h, T) = -\partial F(h, T)/\partial h$.

The temperature T is normalized by the SDW temperature $T_{\rm SDW}$.

4. Numerical results at $T = 0$

The results of our full quantum mechanical calculations are summarized in figures 2(a) for X = ClO_4 and 2(b) for X = NO_3. The curves labelled with $\Delta = 0$ correspond to the normal metallic state for $T_{\rm SDW} < T < T_{\rm AO}$, and those labelled with $\Delta = 0.03$ correspond to the SDW state for $T < T_{\rm SDW}$. It is seen from figure 2(a) that the thermodynamic oscillation of M is absent in the normal metallic state ($\Delta = 0$) for X = ClO_4. This means that it is confined to the SDW state. The oscillation with the same frequency observed in $\rho(H)$ is attributed to the Stark quantum interference oscillation characterized by a simple sinusoidal wave form. In the SDW state ($\Delta \neq 0$), $M(h)$ vigorously oscillates, and its frequency $f_{\rm RO}$ is found to be nearly 0.075. The closed-orbit areas shown using broken lines in figure 1(c) coincide precisely with $f_{\rm RO}$. In the real system, those closed-orbit areas correspond to 260 T. Thus, the rapid oscillation in the thermodynamics quantities is the usual dHvA oscillation caused by the magnetic breakdown orbit shown using broken lines in figure 1(c). The oscillation wave form contains many higher harmonics and is far from a simple sinusoidal one.

These features are contrasted with those for X = NO_3 in figure 2(b), where the thermodynamic oscillation appears both in the normal ($\Delta = 0$) and SDW ($\Delta \neq 0$) states. The two frequencies are the same ($f_{\rm RO} \simeq 0.055$), and $f_{\rm RO}$ is in agreement with the electron or hole closed-orbit areas in figure 1(b) and the closed-orbit areas shown using broken lines in figure 1(c). Also for X = NO_3 the rapid oscillation in the thermodynamic quantities is the usual dHvA oscillation due to the electron and hole closed orbits in figure 1(b) or the magnetic breakdown orbits shown using broken lines in figure 1(c). This is consistent with the observation [12] that the frequencies of the normal and SDW states are the same. As h increases, the intensity $A_{\rm RO}(h)$ progressively increases in both the X = ClO_4 and X = NO_3 cases, except for at extremely high fields. This is because the magnetic breakdown becomes possible upon increasing H, and thus the probability of tunnelling across the SDW gaps increases; the magnetic breakdown orbits denoted using broken lines in figure 1(c) execute cyclic motion. The characteristic breakdown field $H_{\rm MB}$ is found understandably to be an increasing function of Δ in our calculations. Thus, $A_{\rm RO}$ is suppressed by increasing Δ. Under a fixed H, as T decreases below $T_{\rm SDW}$, $A_{\rm RO}(T)$ is expected to have a maximum

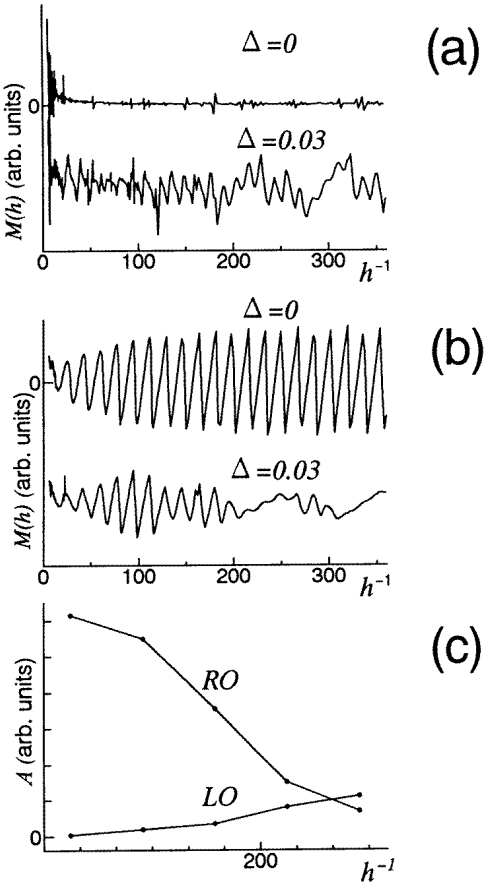

Figure 2. The calculated magnetization $M(h)$ as a function of h^{-1} for the normal metallic state ($\Delta = 0$, upper curve) and the SDW state ($\Delta = 0.03$, lower curve). (a) $\boldsymbol{Q}_a = (0, \pi/b)$ for X = ClO_4 and (b) $\boldsymbol{Q}_a = (\pi/a, 0)$ for X = NO_3. (c) The intensity $A_i(h)$ of the oscillation amplitudes as a function of h^{-1} calculated from (b) for X = NO_3 (i = RO for the rapid oscillation and i = LO for the lower-frequency oscillation). $t_b/t_a = 0.6$, $t_b'/t_a = 0.2$, and $v = 0.2$.

because of the growth of the SDW gap. The rapid oscillation eventually vanishes at lower T where the SDW gap ultimately prevents the rapid oscillation, as we will see in the next section. This explains the mysterious disappearance of the rapid oscillation as observed by Uji *et al* [10]. These behaviours are quite different from those of the ordinary SdH or dHvA oscillations. The SDW gap, in turn, confines the electron motion to the smaller closed orbits shown using bold lines in figure 1(c), giving rise to another oscillation with lower frequency, $f_{\rm LO} \simeq 0.01$, in addition to that with the frequency $f_{\rm RO}$ mentioned above. This frequency corresponds to the small closed orbits. This is clearly seen in the SDW state in figure 2 for both X = ClO_4 and X = NO_3 in the lower-H region. The crossover behaviours of the intensities $A_{\rm RO}$ and $A_{\rm LO}$ are shown in figure 2(c) for X = NO_3. This is precisely what Audouard *et al* [12] found experimentally.

It should be noted that an inverted sawtooth wave form (see figure 2(b)) is obtained for

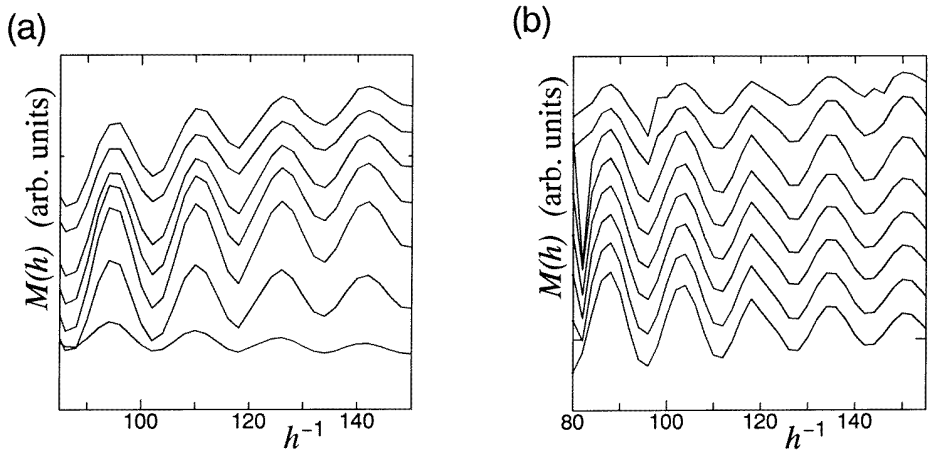

Figure 3. The magnetization $M(h)$ as a function of h^{-1} for various temperatures. $t_b/t_a = 0.6$, $t'_b/t_a = 0.04$, $v = 0.04$, and $\Delta(0) = 0.02$. (a) X = ClO_4 ($T/T_{SDW} = 0.0$, 0.38, 0.63, 0.81, 0.88, 0.94, 0.99 from top to bottom); the oscillation amplitude is non-monotonic in T ($\Delta(0)/T_{SDW} = 5.0$). (b) X = NO_3 ($T/T_{SDW} = 0.0$, 0.40, 0.65, 0.80, 0.85, 0.90, 0.95, 1.00 from top to bottom); the oscillation amplitude increases as T increases ($\Delta(0)/T_{SDW} = 2.0$).

X = NO_3 in which the areas of electron and hole orbits are nearly the same (see figure 1(b)). This inverted form is not explained by the LK formula [20]. We predict that the dHvA sawtooth wave form might be inverted for X = NO_3.

5. The temperature dependence of the rapid-oscillation amplitude

Let us now extend our calculation in the previous section to finite temperatures. The T-dependence of the order parameter $\Delta(T)$ is assumed to be described in the standard mean-field manner, i.e., by the BCS theory. We notice the experimental fact that the BCS relation $\Delta(0)/T_{SDW} = 1.76$ is often violated in low-dimensional conductors because of the fluctuation effects [28] associated with its low dimensionality. Therefore, we regard the ratio $\Delta(0)/T_{SDW}$ as an adjustable parameter in the following.

Examples of $M(h, T)$ oscillation behaviours for selected temperatures are displayed in figure 3(a) for X = ClO_4 and figure 3(b) for X = NO_3. It is directly seen from these examples that the rapid-oscillation amplitude could be non-monotonic in T (figure 3(a)) or could even decrease as T lowers (figure 3(b)), depending on the ratio $\Delta(0)/T_{SDW}$.

The results on the T-dependence of the rapid-oscillation amplitude $A_{RO}(T)$ are shown in figure 4(a) for X = ClO_4 and in figure 4(b) for X = NO_3 for several representative values of $\Delta(0)/T_{SDW}$. For the X = ClO_4 case, the rapid-oscillation amplitude monotonically decreases with increasing T for $\Delta(0)/T_{SDW} = 3.0$, while for $\Delta(0)/T_{SDW} = 5.0$ it exhibits non-monotonic behaviour near T_{SDW}, taking a maximum just below T_{SDW}.

The contrasting T-dependence in these systems is explained as follows: the rapid oscillation comes from the magnetic breakdown orbit blocked by the anion-ordering gap and the SDW gap as we have already pointed out. As $\Delta(T)$ decreases upon increasing T, the SDW gap becomes narrower, thus making the magnetic breakdown easier. This in turn leads to the increasing of the rapid-oscillation amplitude. That is, the T-dependence is governed by two competing factors: one is the ordinary temperature reduction due to the thermal

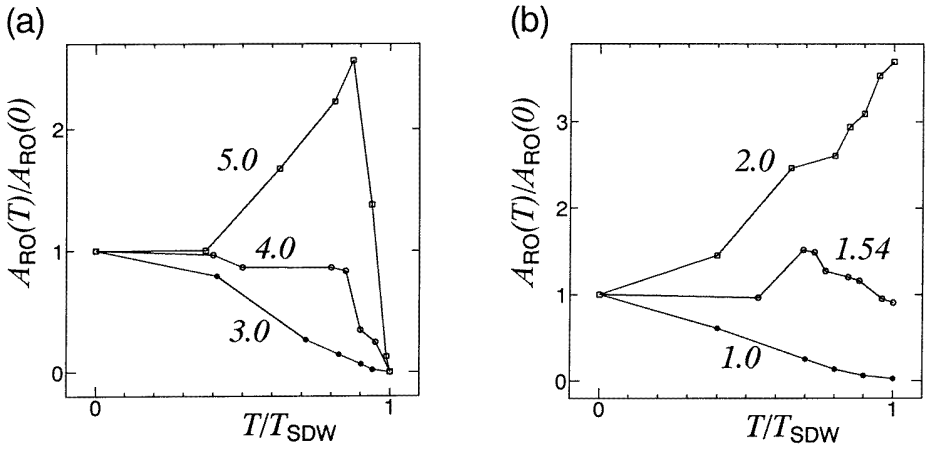

Figure 4. The temperature dependence of the rapid-oscillation amplitude $A_{RO}(T)$ for several values of $\Delta(0)/T_{SDW}$, as indicated. (a) X = ClO_4 and (b) X = NO_3. $t_b/t_a = 0.6$, $t'_b/t_a = 0.04$, $\Delta(0) = 0.02$, and $v = 0.04$.

broadening of the Landau bands and the other is the magnetic-breakdown-enhancement effect due to the gap narrowing. These two factors give rise to the non-monotonic T-dependence for a larger $\Delta(0)/T_{SDW}$ ratio, because on approaching T_{SDW} from below, the SDW gap quickly closes, enhancing the magnetic breakdown. It should be noted that $A_{RO}(T_{SDW}) = 0$ at $T = T_{SDW}$, above which there is no magnetic breakdown orbit available (see figure 1(b) for X = ClO_4).

For the X = NO_3 case, it is seen from figure 4(b) that $A_{RO}(T)$ increases monotonically for $\Delta(0)/T_{SDW} = 2.0$. This can be understood by noting that the gap-narrowing effect overcomes the thermal reduction factor. Note also that $A_{RO}(T = T_{SDW}) \neq 0$, because even above T_{SDW} there exist the magnetic breakdown orbits (see figure 1(b) for X = NO_3). A non-monotonic behaviour of $A_{RO}(T)$ is obtained when $\Delta(0)/T_{SDW}$ becomes smaller, as seen from figure 4(b) for $\Delta(0)/T_{SDW} = 1.54$. The subtle interplay of the two competing factors mentioned above results in a T-dependence which exhibits a maximum below T_{SDW}.

6. Discussions and summary

We have resolved the two main mysteries associated with the rapid-oscillation phenomena in $(TMTSF)_2X$. The subtle interplay between the anion and SDW orderings produces a rich and novel quantum magnetic oscillation under extreme conditions of high H and low T. Although the chosen system parameters are exaggerated a little for ease of computation, the essential features of the Fermi surface topology—which is decisive for magnetic oscillations—are preserved.

6.1. $(TMTSF)_2ClO_4$

(1) In the normal state, whose Fermi surface is shown in figure 1(b), there exists no closed orbit; thus there is no rapid oscillation in thermodynamic quantities such as the magnetization. This is confirmed by the present calculation.

(2) In a real system, a pair of parallel Fermi surfaces whose area corresponds to $F_{\mathrm{RO}} = 260$ T is an ideal situation for Stark quantum interference oscillations in transport quantities, e.g. $\rho(H)$, as is indeed observed experimentally. This identification is consistent with the sinusoidal oscillation wave form observed for the normal state [10].

(3) In the FISDW state above the threshold field $H \sim 5$ T at low temperatures, the SDW nesting induces the possible closed orbits shown in figure 1(c). The approximate area produced is the same as that given above. The rapid oscillation whose frequency corresponds to 260 T becomes possible because of the magnetic breakdown through the blocked SDW gaps in a real system. That is, the rapid oscillation in the thermodynamic quantities is the usual dHvA oscillation. This is why the rapid oscillation in thermodynamic quantities is confined to the FISDW phase, consistently with the existing experiments. Note that the change of the oscillation wave form [10] from a simple sinusoidal one for the normal state to one including higher harmonics for the FISDW state is consistent with our identification.

(4) The rapid oscillation of $\rho(H)$ in the FISDW is complicated to interpret, because on the Fermi surface there are pairs of Fermi surfaces of two different kinds, each consisting of either parallel or anti-parallel lines. The rapid oscillation in $\rho(H)$ contains inevitably two kinds of oscillation each arising either from the Stark quantum interference or from the dHvA oscillation. These different kinds of oscillation contribute collectively to the rapid oscillation of $\rho(H)$. We point out that even when crossing the FISDW–normal boundary by changing either H or T, the rapid-oscillation amplitude varies smoothly, indicating that the oscillation phase of the Stark quantum interference and that of the dHvA oscillations coincide—otherwise the rapid-oscillation wave form would be discontinuous there.

(5) Depending on the ratio $\Delta(0)/T_{\mathrm{SDW}}$, the T-dependence of the Fourier-transformed amplitude of the rapid oscillation could be non-monotonic. The ultimate origin of these non-trivial T-dependences in the Stark quantum interference, and the SdH and dHvA phenomena lies in the fact that the rapid oscillation is due to the magnetic breakdown orbit across the T-dependent SDW gaps. The T-dependence of the Fourier-transformed amplitude of the rapid oscillation exhibits a maximum at $\sim$2 K in $\rho(H)$ and the specific heat [9], while those for the sound velocity [7] and the magnetization are described by a monotonically decreasing function with increasing T. It should be noted that the detailed T-dependences of these individual quantities are determined by the subtle balance between the aforementioned two factors.

(6) The area of the magnetic breakdown orbit depicted using broken lines in figure 1(c) changes slightly in the FISDW phase, since the SDW nesting vector varies as a function of the magnetic field. The phase of the oscillation of its orbit may be affected by this change too. In this paper, since we fix the SDW nesting vector, our discussions are strictly valid only for the $N = 0$ subphase. However, we believe that our calculation may be applicable for the $N \neq 0$ subphases.

(7) It might be of interest to note that the oscillation wave form in figure 2(b) has an inverted sawtooth shape, which is unusual [20]. According to our experience this arises whenever electron and hole orbits with similar sizes exist simultaneously. This reminds us of the dramatic wave-form change, from the regular to the inverted sawtooth shape, that occurs upon crossing the unidentified phase transition line ($T \sim 3$ K and $H \sim 25$ T) for X = ClO_4 observed by McKernan *et al* [29]. Through the analysis of the oscillation wave form it is possible to extract further information on the detailed Fermi surface topology, and to detect the transition line. We suggest that the observed drastic change from the regular to inverted sawtooth wave form upon lowering T for X = ClO_4 above $H \sim 20$ T might be associated with the drastic Fermi surface change.

6.2. (TMTSF)$_2$NO$_3$

(1) As is seen from figure 1(b), there exist the closed electron and hole orbits with equal areas on the Fermi surface in the normal state. The area corresponds to $F_{\mathrm{RO}} = 260$ T in a real system. Thus the rapid oscillation in $\rho(H)$ is due to the ordinary SdH effect.

(2) In the SDW state the SDW nesting produces additional small orbits, which give rise to a slow oscillation with $F_{\mathrm{LO}} = 67$ T in a real system. The rapid oscillation comes about via the magnetic breakdown through the SDW gaps under a strong field.

(3) The reorganized Fermi surface under the SDW-gap formation consists of a pair of parallel and anti-parallel Fermi surfaces, and is very similar to what is obtained for X = ClO_4 in this respect. The magnetoresitance contains both SdH and Stark quantum interference oscillations.

(4) Depending on the ratio $\Delta(0)/T_{\mathrm{SDW}}$, the T-dependence of $A_{\mathrm{RO}}(T)$ could exhibit a maximum. The reason for this is the same as in the case of X = ClO_4.

6.3. Differences between the cases with X = ClO$_4$ and X = NO$_3$

The important difference between the two systems lies in the fact that for X = ClO_4 the successive first-order transitions of the FISDW subphases prevent the remaining closed orbits from undergoing Landau quantization. The subphase transition occurs so as to prevent the Landau band from crossing the Fermi level. This results in a gain in condensation energy via adjustment of the nesting vector. This inhibits the SdH and dHvA oscillations, implying that the low-frequency oscillation should not be observed for X = ClO_4. This contrasts with the X = NO_3 case, for which the low-frequency oscillation with $F_{\mathrm{LO}} = 67$ T corresponding to the electron and hole pockets remaining is observed, because here there is no fine tuning of the SDW nesting vector, and the FISDW seems not to occur. The absence (X = ClO_4) and presence (X = NO_3) of the low-frequency oscillations coincides with observations.

The T-dependences of the rapid oscillations are different for X = ClO_4 and X = NO_3. In the latter case the rapid oscillation should be observed above $T_{\mathrm{SDW}} \sim 12$ K in principle; it may, however, be hard to see it, simply because the temperature is too high. In fact, rapid oscillation in $\rho(H)$ is not observed above 12 K [12], probably because of the thermal smearing effect. Observation of rapid oscillations in thermodynamic quantities for X = NO_3 is quite keenly awaited, and Naughton *et al* [30] have in fact observed them in magnetization measurements. We anticipate unusual T-dependences, some of which are shown in figure 4(b) as examples. For X = ClO_4, the rapid oscillation in the thermodynamic quantities is strictly confined to the FISDW phase. This should be tested experimentally. In various thermodynamic measurements [6–9], the absence of any rapid oscillation above the FISDW transition temperature, both for T-sweeping and for H-sweeping, has been reported.

6.4. Future studies and remaining problems

So far we have discussed rapid oscillation due to anion ordering. For X = PF_6 and X = AsF_6 where anion ordering is absent, rapid oscillation is still observed, for which we have no explanation.

We identify the rapid oscillation of the normal state with X = ClO_4 as Stark quantum interference. Uji *et al* [10] observed this in $\rho_{xx}(H)$, but not in $\rho_{zz}(H)$. This coincides with the above identification, because a pair of open Fermi surfaces runs along the x-axis. McKernan *et al* [29] report a conflicting result: they observe rapid oscillation in $\rho_{zz}(H)$. Both experimentally and theoretically, the Stark quantum interference deserves further study.

McKernan *et al* [29] also present a new phase diagram in the T–H plane for X = ClO_4. The high-field and low-T region is occupied by yet another new kind of SDW subphase: SDW_1 and SDW_2. In view of the present study we suggest that the detailed investigation of the rapid oscillation provides important information on the reconstructed Fermi surfaces in each subphase, since the rapid oscillation in thermodynamic quantities is ultimately a dHvA effect, which is best suited for investigating the 'fermiology'. It is interesting to point out in this respect that the inverted sawtooth wave form of the rapid oscillation in the magnetization measurement found by McKernan *et al* [29] corresponds to SDW_2, not to SDW_1. Shi *et al* [7] previously observed a similar unexpected oscillation phase change by a half-period in their sound velocity measurements in exactly the same H- and T-region, which is certainly related to the inversion of the oscillation wave form mentioned above.

The system with X = NO_3 is the best system on which to test our proposals. First of all, the rapid oscillation in thermodynamic quantities must be observed both in the normal and SDW states [30]. Secondly, the H- and T-dependences of the Fourier-transformed amplitude should be investigated, to enable us to compare them with the already known counterpart in $\rho(H)$. It is highly likely that the T-dependence of the Fourier-transformed amplitude exhibits a maximum. We anticipate that the rapid-oscillation wave form must be an inverted sawtooth one.

It should be noticed that the present nesting vector $\boldsymbol{Q}_{\mathrm{SDW}} = (\pi/a, \pi/b)$ has been accepted as the optimal one; it may be, however, different if we take the anion ordering into account more seriously. The optimization of the nesting vector for X = ClO_4 is still an open problem.

Acknowledgments

We thank S Uji, K Oshima, T Osada and S Kagoshima for useful discussions.

Note added in proof. As pointed out by Uji *et al* [31], the rapid oscillation for X = PF_6 can be understood as arising from the reorganization of the Fermi surfaces due to the SDW, because the nesting vector is nearly equal to $(\pi/a, \pi/2b)$. The resulting Fermi surfaces are the same as those in the SDW state for X = ClO_4 and X = NO_3, leading to rapid oscillation without anion ordering. The major mysteries of the rapid oscillation in (TMTSF)$_2$X are all resolved.

References

[1] See, for a review,
Ishiguro T and Yamaji K 1990 *Organic Superconductors* (Berlin: Springer)
[2] Gorkov L P and Lebed A G 1984 *J. Physique Lett.* **745** L433
Montambaux G, Héritier M and Lederer P 1985 *Phys. Rev. Lett.* **55** 2078
Yamaji K 1985 *J. Phys. Soc. Japan* **54** 1034
Maki K 1986 *Phys. Rev.* B **33** 4826
Osada T, Kagoshima S and Miura N 1992 *Phys. Rev. Lett.* **69** 1117
Machida K, Hori Y and Nakano M 1993 *Phys. Rev. Lett.* **70** 61
Machida K, Hasegawa Y, Kohmoto M, Yakovenko V M, Hori Y and Kishigi K 1994 *Phys. Rev.* B **50** 921
[3] Ulmet J P, Auban P, Khmou A and Askenazy S 1985 *J. Physique Lett.* **46** L535
[4] Ulmet J P, Khmou A, Auban P and Bachere L 1986 *Solid State Commun.* **58** 753
[5] Osada T, Minura N and Saito G 1986 *Solid State Commun.* **60** 441
[6] Yan X, Naughton M J, Chamberlin R V, Chiang L Y, Hsu S Y and Chaikin P M 1988 *Synth. Met.* **27** B145
Yan X, Naughton M J, Chamberlin R V, Hsu S Y, Chiang L Y, Brooks J S and Chaikin P M 1987 *Phys. Rev.* B **36** 1799
[7] Shi X D, Kang W and Chaikin P M 1994 *Phys. Rev.* B **50** 1984
[8] Yu X, Chiang L, Upasani R and Chaikin P M 1994 *Phys. Rev. Lett.* **65** 2458

[9] Fortune N A, Brooks J S, Graf M J, Montambaux G, Chiang L Y, Perenboom J A A J and Althof D 1990 *Phys. Rev. Lett.* **64** 2054
[10] Uji S, Terashima T, Aoki H, Brooks J S, Tokumoto M, Takasaki S, Yamada J and Anzai H 1996 *Phys. Rev.* B **53** 14 399
[11] Kang W, Behnia K, Jérome D, Balicas L, Canadell E, Ribault M and Fabre J M 1994 *Europhys. Lett.* **25** 363
[12] Audouard A, Goze F, Dubois S, Ulmet J P, Brossard L, Askenazy S, Tomić S and Fabre J M 1994 *Europhys. Lett.* **25** 363
Audouard A, Goze F, Ulmet J P, Brossard L and Askenazy S 1994 *Phys. Rev.* B **50** 12 726
[13] Kang W, Cooper J R and Jérome D 1991 *Phys. Rev.* B **43** 11 467
Also see
Schwenk H, Parkin S S S P, Schumaker R, Greene R L and Schweitzer D 1986 *Phys. Rev. Lett.* **56** 667
[14] Audouard A, Ulmet J P and Fabre J M 1995 *Synth. Met.* **70** 751
[15] Here we focus solely on these two well-studied systems (those with X = ClO_4 and X = NO_3), which are best suited for our comparative study. Because within the standard model both bands can be regarded as essentially the same for our purposes, we adopt the half-filling notation rather than the usual quarter-filling notation (see [1], p 40).
[16] Shinagawa H, Kagoshima S, Osada T and Miura N 1994 *Physica* B **201** 490
[17] Lebed A G 1995 *Phys. Rev. Lett.* **74** 4903
Lebed A G and Bak P 1989 *Phys. Rev.* B **40** 11 433
Yakovenko V M 1992 *Phys. Rev. Lett.* **68** 3607
Maki K 1992 *Phys. Rev.* B **45** 5111
Montambaux G 1991 *Synth. Met.* **41** 3807
[18] Machida K, Kishigi K and Hori Y 1995 *Synth. Met.* **70** 853
Machida K, Kishigi K and Hori Y 1995 *Phys. Rev.* B **51** 8946
Kishigi K, Nakano M, Machida K and Hori Y 1995 *J. Phys. Soc. Japan* **64** 3043
[19] Kishigi K and Machida K 1995 *J. Phys. Soc. Japan* **64** 3853
[20] Shoenberg D 1984 *Magnetic Oscillation in Metals* (Cambridge: Cambridge University Press)
[21] Pippard A B 1989 *Magnetoresistance in Metals* (Cambridge: Cambridge University Press)
[22] A brief version of this paper:
Kishigi K and Machida K 1996 *Phys. Rev.* B **53** 5461
[23] It is stated [20] that the T-dependence of the oscillation amplitude due to the Stark interference is weak. This statement is correct as regards the general tendency, but depends on the actual Fermi surface situation, and the amplitude could possibly be T-dependent, as in the X = ClO_4 case.
[24] This is proved by the second-order perturbation calculation for V:
Yakovenko V M 1993 *Phys. Rev. Lett.* **70** 2675
[25] Biškup N, Balicas L, Tomić S, Jérome D and Fabre J M 1994 *Phys. Rev.* B **50** 12 721
[26] Basletić M, Biškup N, Korin-Hamzić B, Tomić S, Hamzić A, Bechgaard K and Fabre J M 1993 *Europhys. Lett.* **22** 279
[27] It is interesting to note that in the case of the field-induced SDW for X = ClO_4, the x-component $Q_x = 2k_F + NebH/hc$ of the optimal nesting vector $\boldsymbol{Q}_{SDW} = (Q_x, Q_y)$ depends on the subphase numbering N, and on H (k_F is the Fermi wave number). The deviation from $Q_x = 2k_F = \pi/a$ is of the order of $\phi/\phi_0 = 10^{-2}$–10^{-3} in our field region, and Q_y is also almost independent of H. The observability of the oscillation itself means that the closed-orbit area must be nearly unchanged against H, giving credence to our approximation of the H-independent $\boldsymbol{Q}_s$. We also note here that the area enclosed by the anion ordering does not drastically change even when Q_x varies in order to maximize the condensation energy.
[28] Grüner G 1994 *Density Waves in Solids* (New York: Addison-Wesley)
[29] McKernan S K, Hannahs S T, Scheven U M, Danner G M and Chaikin P M 1995 *Phys. Rev. Lett.* **75** 1630
[30] Recently, in the magnetization for X = NO_3, the rapid oscillation has been confirmed:
Naughton M J, Ulmet J P, Lee I J and Fabre J M 1997 *Synth. Met.* at press
[31] Uji S *et al* 1997 *Phys. Rev.* B submitted